Ocean Sci. Discuss., https://doi.org/10.5194/os-2018-47
Manuscript under review for journal Ocean Sci.
Discussion started: 24 August 2018

Ocean Science
Discussions
Open Access
EGU

Estimation of geostrophic current in the Red Sea based on Sea level anomalies derived from extended satellite altimetry data

Ahmed Mohammed Taqi[a,b], Abdullah Mohammed Al-Subhi[a], and Mohammed Ali Alsaafani[a]
[a]Department of Marine Physics, King Abdulaziz University, Jeddah, Saudi Arabia;
[b]Department of Marine Physics, Hodeihah University, Hodeihah, Yemen

Correspondence to: Ahmed Mohammed Taqi (ataqi@stu.kau.edu.sa)

Abstract

The geostrophic currents data near the coast of the Red Sea has a large gap. Due to that, the sea level anomaly (SLA) data of Jason-2 has been reprocessed and extended towards the coast of the Red Sea and merged with AVISO data at the center of the Red Sea. The processing has been applied to build a data grid to achieve best results for the SLA and geostrophic current. The results obtained from the new extended data at the coast are more consistent with the observed data and hence geostrophic current calculation. The estimated geostrophic current match well with that estimated for observed CTD data. The pattern of SLA distribution and geostrophic currents are divided into two seasons; Winter season extends from October to May and Summer from June to September. The geostrophic currents along the eastern Red Sea flow toward north and southward along the west coast. This flow is modified with the presence of the cyclonic and anticyclonic eddies, which are more concentrated in the central and northern Red Sea. The study has shown anticyclonic eddies (AE) on the eastern side of the Red Sea, but cyclonic eddies (CE) on the west side during Winter. During Summer the (CE) are along the eastern side and (AE) along the western side.

1. Introduction

The Red Sea is a narrow semi-enclosed water body that lies between continents of Asia and Africa. It is located between latitude 12.5°-30°N and longitude 32°-44°E in an NW-SE orientation. Its average width is 220 km and the average depth is 524 m (Patzert, 1974). It is connected at its northern end with the Mediterranean Sea through the Suez Canal and at its southern end with the Indian Ocean through the strait of Bab El- Mandab. The exchange of water through Bab El- Mandab (shallow sill of 137 m) is the most significant factor that determines the oceanographic properties of the Red Sea (Smeed, 2004).

During winter, the southern part of the Red Sea is subject to SE monsoon wind, which is relatively strong from October to December, with a speed of 6.7-9.3 ms^{-1} (Patzert, 1974). During the summer season, the wind is shifting its direction to be from NW. On the other hand, in the northern part of the Red Sea, the dominant wind is NW all year around.

The circulation in the Red Sea is driven by strong thermohaline and wind forces (Neumann and McGill, 1961; Phillips, 1966; Quadfasel and Baudner, 1993; Siedler, 1969; Tragou and Garrett, 1997). Several studies in the Red Sea have focused on thermohaline circulation, where they found that the exchange flow between the Red Sea and Gulf of Aden consists of two layers

Ocean Sci. Discuss., https://doi.org/10.5194/os-2018-47
Manuscript under review for journal Ocean Sci.
Discussion started: 24 August 2018

in winter and three layers in summer through Bab El- Mandab (e.g.Phillips 1966; Tragou and Garrett 1997; Murray and Johns 1997; S. Sofianos and Johns 2015;Al Saafani and Shenoi, 2004; Smeed, 2004). Other studies describe the basin-scale circulation based on modelling approach, usually forced at a relatively low-resolution (1°) by buoyancy flux and global wind (Clifford et al., 1997; Sofianos, 2003; Tragou and Garrett, 1997; Biton et al., 2008; Yao et al., 2014a,b). The horizontal circulation in the Red Sea consists of several eddies, some of them are semi-permanent eddies (Quadfasel and Baudner, 1993), that often present during the winter (Clifford et al., 1997; Sofianos and Johns, 2007) in the northern Red Sea. The circulation system in the central Red Sea is dominated by cyclonic (CE) and anticyclonic eddies (AE), mostly between 18ºNand 24ºN. Eddies are also found in the southern Red Sea but not in a continuous pattern (Johns et al., 1999). Zhan et al., (2014) reported recurring or persistent eddies in the north and the central Red Sea, although there are differences in the number of eddies, their location, and type of vorticity (cyclonic or anticyclonic).

The long-term sea level variability in the Red Sea is largely affected by the wind stress and the combined impact of evaporation and water exchange across the strait of Bab El Mandeb (Edwards, 1987; Sultan et al., 1996). The Sea level in the Red Sea is higher during winter and lower during summer (Edwards, 1987; Sofianos and Johns, 2001; Manasrah et al., 2004). It is characterized by two cycles, annual and semi-annual, where the annual cycle is dominant (Abdallah and Eid, 1989; Sultan and Elghribi, 2003).

In recent years, there has been an increasing interest for using satellite altimetry Sea level anomaly (SLA) which offer large coverage and long data period for providing measurements of SSH, wave height and wind speed (Chelton et al., 2001). However, the altimeter data undergoes several processing stages for corrections due to the atmosphere and ocean effects (Chelton et al., 2001). The satellite altimetric data has been used for the open ocean for a long time with great success, while the data of the coastal region suffers from gaps of almost 50 km form the coastline. The coastal region requires further corrections due to additional difficulties based on the closeness of the land (Deng et al., 2001;Vignudelli et al., 2005; Desportes et al., 2007; Durand et al., 2009; Birol et al., 2010). In the past two decades, many researchers have sought to develop different methods to improve the quality, accuracy and availability of altimetric data near the coast (e.g. Vignudelli et al., 2000;Deng and Featherstone, 2006; Hwang et al., 2006; Guo et al. 2009, 2010; Vignudelli et al., 2005; Desportes et al., 2007; Durand et al., 2009; Birol et al., 2010; Khaki et al., 2014; Ghosh et al., 2015; Taqi et al., 2017). The satellite altimetry faces three types of problems near the coast; (1) the echo interference with the surrounding ground as well as the inland water surface reflection (Andersen and Knudsen, 2000; Mantripp, 1966), (2) environmental and geophysical corrections such as dry tropospheric correction, wave height, high frequency and tidal corrections from global models, etc. and (3) spatial and temporal corrections during sampling (Birol et al., 2010).

The ocean currents circulate water worldwide. They have significant influence on the transfer of energy and moisture between the ocean and the atmosphere. Ocean currents play a significant role in climate change in general. In addition, they contribute to the distribution of hydrological characteristics, nutrients, contaminants and other dissolved materials between the coastal and the open areas, and among the adjacent coastal regions. Ocean currents carry sediment from and to the coasts, so play a significant role in shaping of the coasts. That is important in the coastal region where in the densely inhabited coastal region, producing large amounts of pollutants. Understanding of the currents helps us in dealing with the pollutants and coastal management.

Ocean Sci. Discuss., https://doi.org/10.5194/os-2018-47
Manuscript under review for journal Ocean Sci.
Discussion started: 24 August 2018

The objective of the present research is to study the geostrophic current in the Red Sea including the coastal region using the modified along track Jason-2 SLA along the coast produced by Taqi et al., (2017).

2. Material and Methods

2.1. Description of data

2.1.1 Fourier series model (FSM) SLA

The SLA data used in this study is weekly Jason-2 along the track from June 2009 (cycle 33) to October 2014 (cycle 232) which has been extended to the coastal region by Taqi et al., (2017) by applying the FSM method. The extended data shows a good agreement with the coastal tide gauge station data. In brief, the FSM method of extending SLA consists of four steps; the first step is the removal from SLA the outliers which are outside three times standard deviation from mean. Second step; the SLA is recomputed using Fourier series equation along the track. Third step; the data is then filtered to remove the outliers in the SLA with time similar to the first step. Finally, the SLA data is linearly interpolated over the time to form the new extended data which is called FSM. For more details on the FSM method, refer to Taqi et al., (2017).

2.1.2 AVISO, Tide Gauge, and hydrographic datasets

This study uses two types of SLA data; The first set is the (SLA), which has been downloaded from the Archiving Validation and Interpretation of Satellite Oceanographic (AVISO) (ftp://ftp.aviso.altimetry.fr/global/delayed-time/grids/msla/all-sat-merged). The second dataset is the SLA from the extended FSM data. The temperature and salinity profiles used for geostrophic estimation are received from three cruises, 1-during March 16 to 29, 2010 onboard R/V Aegaeo, 2-during April 3 to 7, 2011 onboard Poseidon and 3- during October 16 to 19, 2011 onboard same ship. Finally, three tide gauges data at the eastern coastline of the Red Sea are obtained from the General Commission of Survey (SGS) at the Kingdom of Saudi Arabia (Figure1) and their location details are shown in Table (1).

2.2 Method

The SLA data used in this study are coming from two sources: (1) the FSM data near the coast and (2) the AVISO data along the axis of the Red Sea. The steps to merge the two datasets and calculating the geostrophic currents are given below.

First, the along-track FSM data are used to produce gridded data to a spatial resolution of ¼° × ¼° for the comparison with Aviso data. The second step, the coastal FSM gridded data then combined with AVISO offshore data, to produce combined ¼° × ¼° SLA data extended toward the coast (here and after will be called FSM-SLA). Finally, surface geostrophic currents are estimated from FSM-SLA data using the following equation;

$$u_g = -\frac{g}{f}\frac{\partial \zeta}{\partial y} \qquad v_g = \frac{g}{f}\frac{\partial \zeta}{\partial x} \qquad (2)$$

Ocean Sci. Discuss., https://doi.org/10.5194/os-2018-47
Manuscript under review for journal Ocean Sci.
Discussion started: 24 August 2018

Where (u_g, v_g) is the surface geostrophic current, g is gravity, f is the Coriolis parameter and ζ is the sea surface height.

The estimation of geostrophic currents from CTD data is using the following equation;

$$u_g = -\frac{1}{f\rho}\frac{\partial p}{\partial y} \qquad v_g = \frac{1}{f\rho}\frac{\partial p}{\partial x} \qquad (2)$$

where ρ is the density of seawater, p is hydrostatic pressure derived from the density. The reference level to estimate the geostrophic current from CTD data was the depth of 700 m similar to that used by Sultan and Ahmad (1990).

Table 1The location of tide gauge stations and period of measurement.

Station	Latitude	Longitude	Period
Jazan	16.87	42.55	1/9/2012 to 31/8/2013
Jeddah	21.42	39.15	1/9/2012 to 31/8/2013
Yanbu	23.95	38.25	1/9/2012 to 31/8/2013

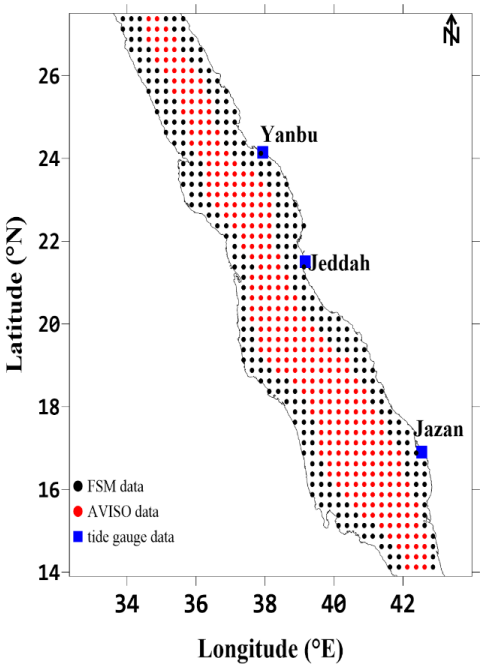

Figure (1) show the study area and the grid-points locations with a spatial resolution of ¼° × ¼° and locations of the tide gauges. Correspondence to: Ahmed. M. Taqi (ataqi@stu.kau.edu.sa)

3. Result and Discussion

The statistical analysis has been conducted to show the quality of FSM-SLA as compared with AVISO. The Correlation Coefficient (CC) reveals a good agreement between the two datasets

Ocean Sci. Discuss., https://doi.org/10.5194/os-2018-47
Manuscript under review for journal Ocean Sci.
Discussion started: 24 August 2018

in the open sea (about 0.7 to 0.9) and is shown in figure 2. Near the coasts, on the other hands, shows weak CC between the two data sets; 0.45 to 0.7.

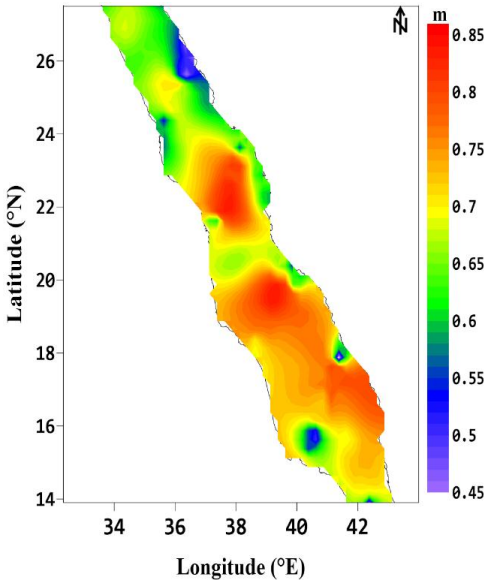

Figure (2) show the correlation coefficient between AVISO and FSM data

Furthermore, the observed SLA from the coastal tide gauge is compared with the FSM-SLA data and AVISO datasets. Table (2) illustrates some of the statistical analysis, where the root mean square error (RMSE) is lower for FSM-SLA as compared to that of AVISO.

Table (2) statistical analysis for AVISO and FSM-SLA data with observed data (in 2013).

	Jasan		Jeddah		Yanbu	
	FSM-SLA	AVISO	FSM-SLA	AVISO	FSM-SLA	AVISO
CC	0.936	0.914	0.915	0.906	0.907	0.895
RMSE(m)	0.073	0.085	0.069	0.094	0.067	0.104
Note: The p-value corresponding to all comparison is very low (P<0.0001), indicating that the results from correlation are significant.						

Figure 3 shows the SLA time series for 2013 from the three coastal stations as compared with the FSM-SLA and AVISO. The three stations datasets have similar seasonal pattern and FSM-SLA coincides with observed SLA in shorter-duration fluctuations. This agreement is clearly shown in Table 2. The comparison of FSM-SLA data and the observed SLA data (at Jazan, Jeddah, and Yanbu stations) show a better correlation than between the AVISO and observed SLA data as shown in figure3 and table.2.These CC differences indicate that the FSM-SLA shows better

Ocean Sci. Discuss., https://doi.org/10.5194/os-2018-47
Manuscript under review for journal Ocean Sci.
Discussion started: 24 August 2018

accuracy near the coast. These results were consistent with those obtained for along-track Jason-2 SLA with coastal stations by Taqi et al., (2017).

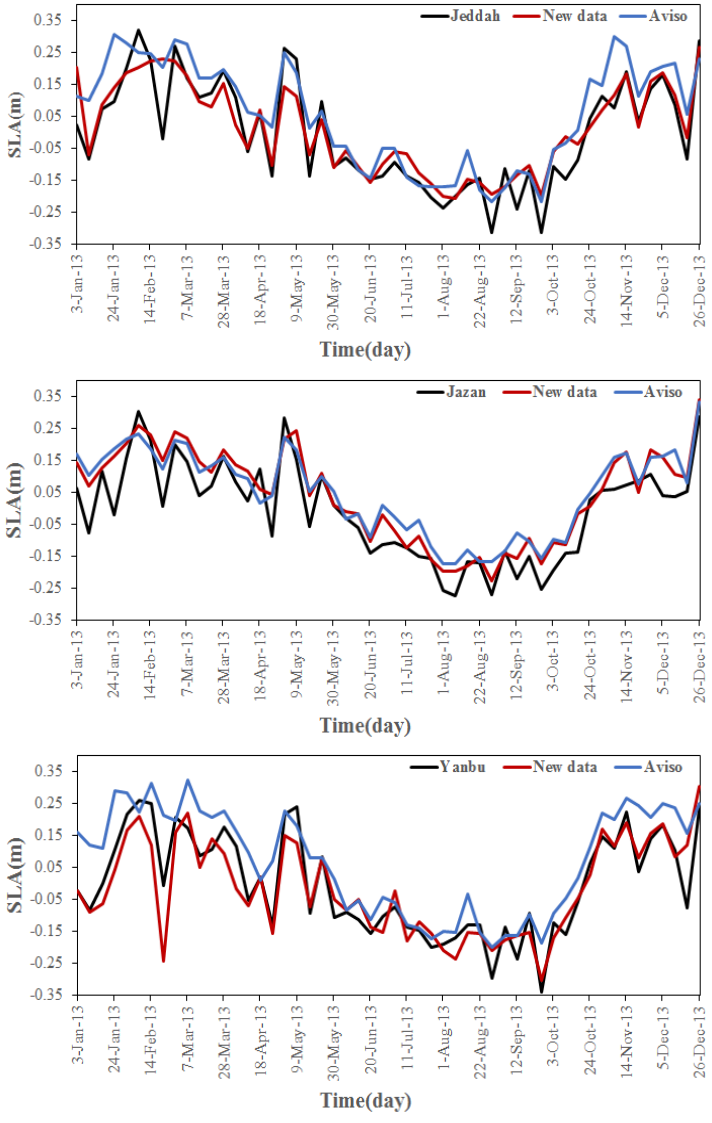

Figure 3. Comparison of Aviso (blue)

Figure 4 shows a comparison between the geostrophic currents for the central Red Sea derived from AVISO and FSM-SLA for three different times (March 2010, April 2011, and October 2011), those different periods corresponding to the timing of three cruises described in section 2.1.

Ocean Sci. Discuss., https://doi.org/10.5194/os-2018-47
Manuscript under review for journal Ocean Sci.
Discussion started: 24 August 2018

164 It can be seen from the figures 4(b,d,f) that there is a significant matching in the directions
165 of geostrophic currents from FSM-SLA with CTD data near the coast and off shore. This result is
166 in agreement with Bower and Farrar (2015) findings, especially in October 2011 (figure 4f).
167 However, the directions of geostrophic currents from AVISO and the CTD data are not always
168 matching. To illustrate, in October 2011, the direction from AVISO is in the opposite direction
169 from CTD data.

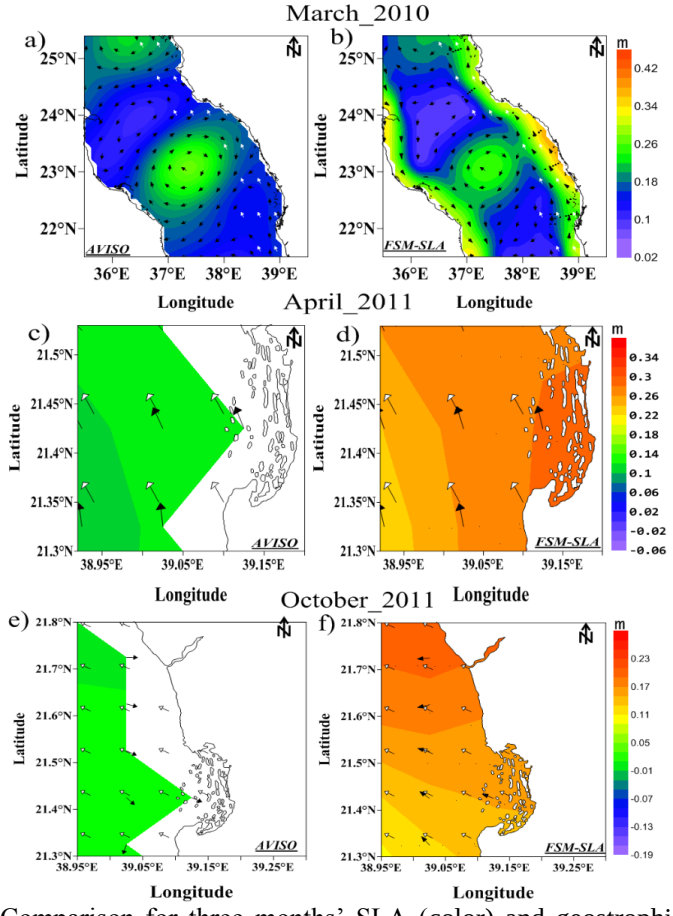

170 Figure (4) Comparison for three months' SLA (color) and geostrophic currents (black
171 vectors) between (left) AVISO and (right) FSM-SLA white vectors show geostrophic currents
172 from CTD data.

173 In March 2010 the geostrophic currents along the eastern coast of the Red Sea are towards
174 the north for both FSM-SLA and AVISO, except between 22.2˚ – 23˚N, where the FSM-SLA and
175 CTD data geostrophic currents are in the same direction while AVISO geostrophic current is in
176 the opposite direction (see figure 4a,4b).

177 Figure 5 shows monthly climatology variation for the 6-year period for SLA and
178 geostrophic current. The SLA is higher during the period from October to May and lower during
179 rest of the year, this pattern is consistent with previous studies (Patzert, 1974; Edwards, 1987;

Ocean Sci. Discuss., https://doi.org/10.5194/os-2018-47
Manuscript under review for journal Ocean Sci.
Discussion started: 24 August 2018

Ahmad and Sultan, 1989; Sofianos and Johns, 2001; Sultan and Elghribi, 2003;Manasrah et al., 2004, 2009). Based on calculations made here, the geostrophic current of Red Sea along the eastern coast is northward while along the western coast is southward. This northward flowing current is consistent with a previous study by Bower and Farrar (2015). Similar results are also obtained from three-dimensional modeling by (Clifford et al., 1997; Eshel and Naik, 1997; Sofianos, 2003, 2002). The figure presents the surface circulation during January in the northern part, where two eddies formed between 25° – 27.5°N. The first eddy is an anticyclone between 26.3° – 27.5°N on the eastern side of the Red Sea. The other eddy is cyclonic located between 25° – 26.3°N near the western coast. To the south of that, there are two other eddies between 22.5° – 24.7°N, cyclonic on the western side and anticyclonic on the eastern side. These results match those observed in previous studies by (Eladawy et al., 2017; Sofianos and Johns, 2003). Two cyclonic eddies and an anticyclonic eddy found at 19.5° – 22.5°N are consistent with those modeled by Sofianos and Johns, (2003). Near Bab al-Mandab, there is a cyclonic eddy on the western side between 15° – 16.5°N.

In February, the surface circulation of the Red Sea is similar to that during January, with some differences in the eddies structure. The anticyclonic eddy near 27°N on the eastern sides of the Red Sea starts shifting toward the western coast, while a cyclonic eddy at 25° – 26.3° N start appearing. The cyclonic eddies between 22.5° – 24.7°N on the western side are less clear in this month.

In March and April, all the eddies are located along the central axis of the Red Sea. In the north, the anticyclonic eddy near 27°N is shown in both months, while the cyclonic eddy is not clear during March and April. The anticyclonic eddy shown near23°to 24 °N during March is weakening during April.

In May, there is no clear eddy between 27.5°N and 25°N. However, four eddies are clearly existing between 19.5° –25°N; two cyclonic eddies at 24° – 25°N, and 20° – 22°N, two anticyclonic eddies at 23° – 24°N, and 19.5° – 20°N. From the previous results, it can be seen several cyclonic and anticyclonic eddies distributed all over the Red Sea and these results match those in modelling studies (Clifford et al., 1997; Eladawy et al., 2017; Sofianos, 2003, 2002, Yao et al., 2014a)

During June, the flow of the geostrophic currents in the northern part reversed its direction. This accompanies a formation of large cyclonic eddy extending from 25.5°– 27.5°N occupying the entire width of the Red Sea. To the south of it, another cyclonic eddy observed between 24° – 25°N and an anticyclonic eddy between 23° – 24°N are also noticed during June with a similar strength during May. The cyclonic eddy seen between 17° – 20°N during May, is also seen during this month with more strength. To the south of it, the flow is towards the Bab el-Mandab following normal summer pattern. The flow pattern along the coast is similar to results of (Chen et al., 2014) for winter (January to April). The short-term climatology of geostrophic current in the Red Sea is

Ocean Sci. Discuss., https://doi.org/10.5194/os-2018-47
Manuscript under review for journal Ocean Sci.
Discussion started: 24 August 2018

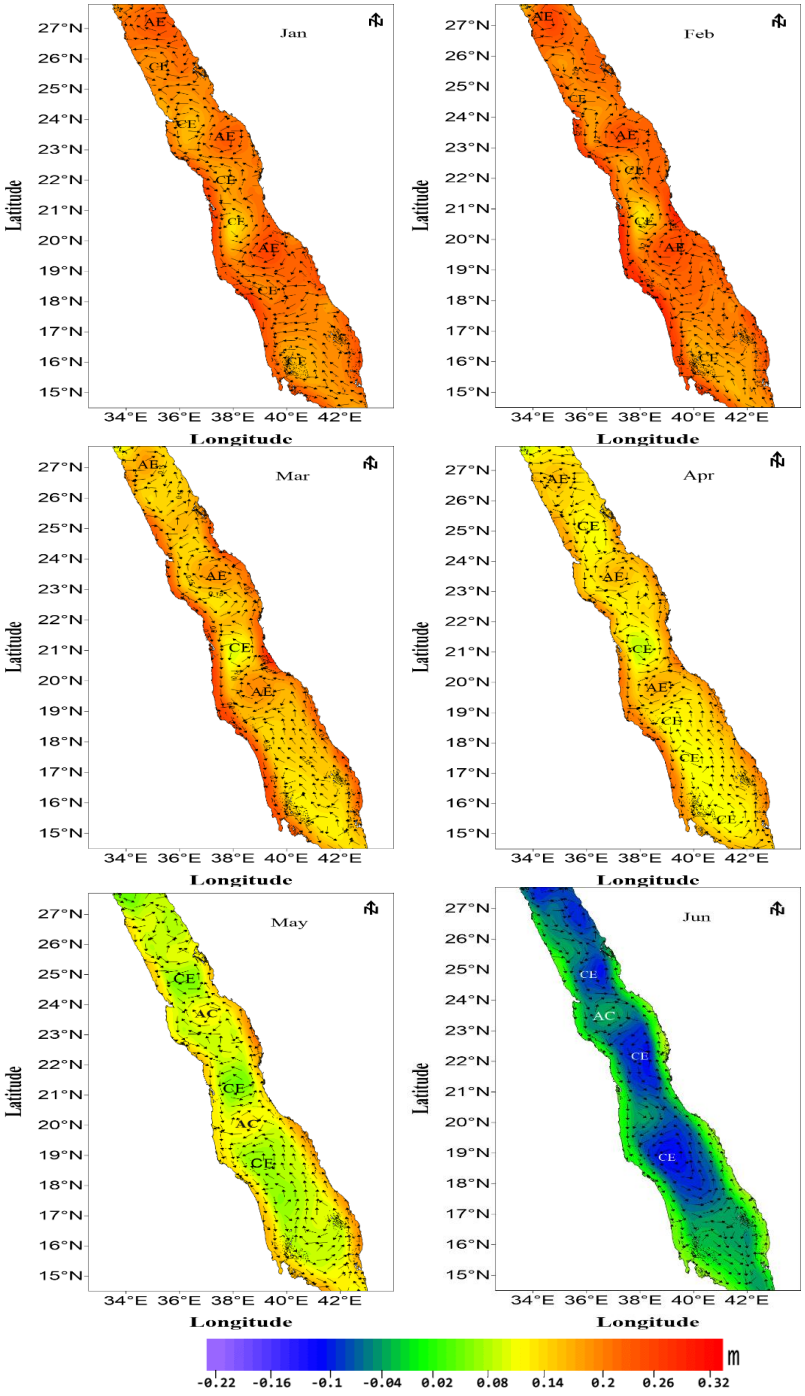

Figure 5 shown monthly climatology for geostrophic current and Sea level anomaly (Reference current length =0.5m/s)

Ocean Sci. Discuss., https://doi.org/10.5194/os-2018-47
Manuscript under review for journal Ocean Sci.
Discussion started: 24 August 2018

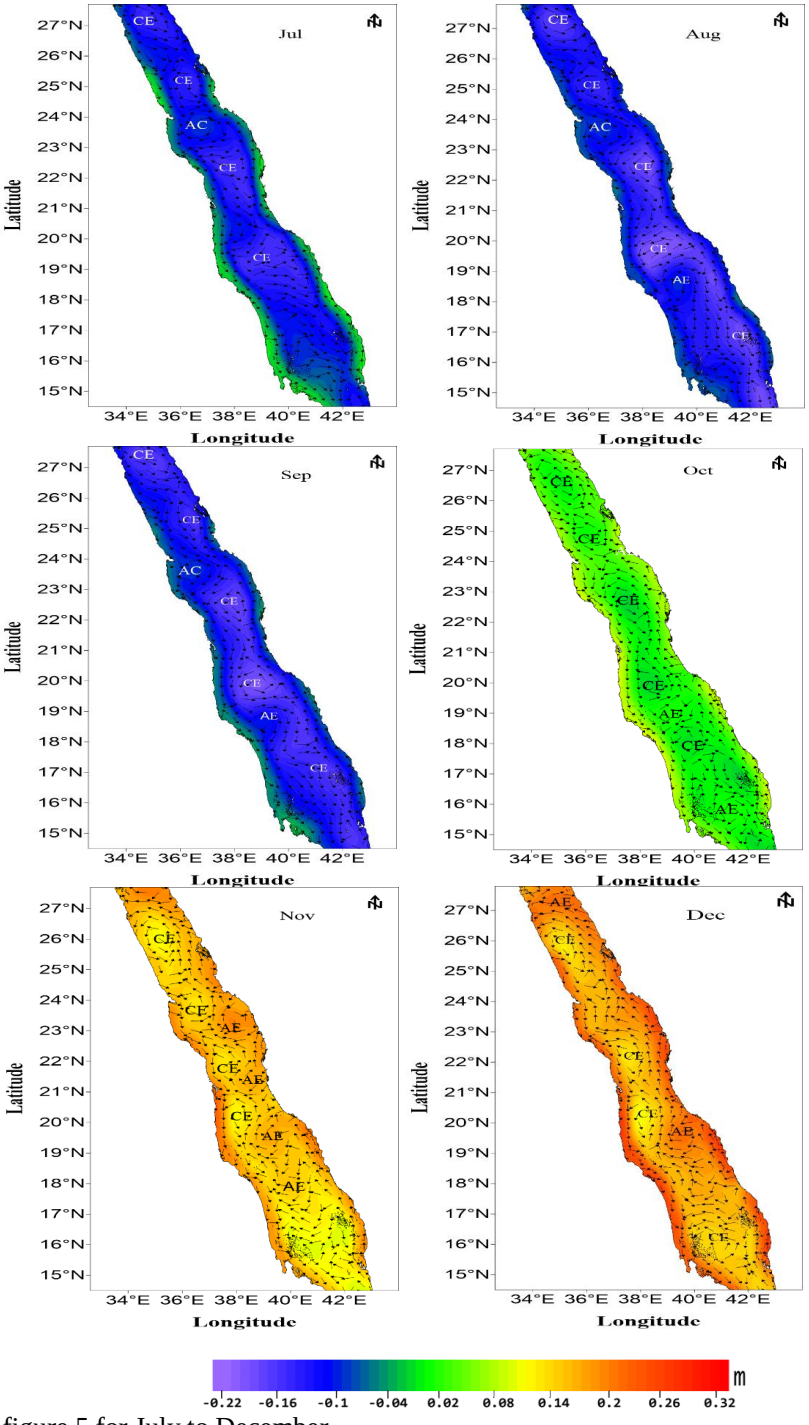

218 Figure 6 As figure 5 for July to December

Ocean Sci. Discuss., https://doi.org/10.5194/os-2018-47
Manuscript under review for journal Ocean Sci.
Discussion started: 24 August 2018

dominated by cyclonic and anticyclonic eddies all over the Red Sea, and especially in the central and northern parts of the sea.

During July-September, the flow of the geostrophic currents structure is similar to that of June with two cyclonic eddies north of 24.5°N and anticyclonic eddy between 23° – 24°N. South of these two eddies, another cyclonic eddy extends to 19°N; to the south of that, there is an outflow towards the south all over the width of the Red Sea with narrow inflow along the eastern coast of the Red Sea. These results are consistent with data obtained by(Clifford et al., 1997; Eladawy et al., 2017; Sofianos, 2003, 2002, Yao et al., 2014b)

During summer (June-September), the changes in wind speed and direction cause reversed of changes in the direction of flow consequently, the locations of eddies are also changed (Chen et al., 2014). The surface current flows from the Red Sea to the Gulf of Aden through the Bab-el-Mandeb. The anticyclonic eddy shown in the north at 27.5°N in winter is replaced with cyclonic eddy, during this season. Summer is dominated by cyclonic eddies as shown in figure 6.

During October, the geostrophic current is weak as compared with that during September, still cyclonic but with less strength. The anticyclone seen during September between 23° – 24°N is not clear during October. In the central and southern parts, the flow of the geostrophic currents is towards south along the western coast and towards the north along the eastern side with the presence of cyclonic and anticyclonic eddies in the central axis of the Red Sea with a weak flow. In November and December, the structure of geostrophic currents are similar to that of October but with stronger currents and well established cyclonic and anticyclonic eddies.

During summer, the cyclonic eddies are often concentrated on the west side and the anticyclonic eddies on the eastern side of the Red Sea, while in winter it is the opposite. Their formation might be related to wind forces and thermohaline (Neumann and McGill, 1961; Phillips, 1966; Quadfasel and Baudner, 1993; Siedler, 1969; Tragou and Garrett, 1997).

Ocean Sci. Discuss., https://doi.org/10.5194/os-2018-47
Manuscript under review for journal Ocean Sci.
Discussion started: 24 August 2018

Figure (7) shows the general schematic for the climatology derived from 6 years for the geostrophic current, which shows inflow toward the Red Sea through the Bab El- Mandab along the western side to 15.5°N, this result is in agreement with Sofianos and Johns, (2003). The flow continued towards the north along the eastern side to the northern Red Sea. There is a cyclonic eddy in the western side of the Red Sea between 15°N and 18°N. To the north of this eddy another cyclonic eddy is located between 18°N and 21°N. While in the northern part of the Red Sea between 23°N and 28°N a cyclonic eddy is dominant.

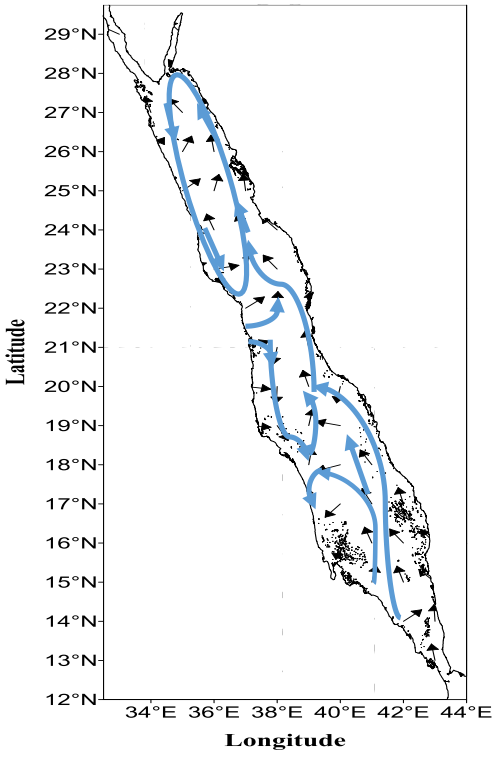

Figure 7 Annual average surface geostrophic currents, black arrows are actual surface geostrophic currents and blue arrows are schematic streamline.

4. Conclusion

In general, the geostrophic current has been estimated from FSM-SLA for Red Sea region, and the distribution of the geostrophic current shows that the winter period extends from October to May and summer period extends from June to September. This pattern is similar to that shown by (Sofianos and Johns, 2001).

The geostrophic current along the eastern coast is towards the north and southward along the western coast of the sea. While the eddies are concentrated in the northern Red Sea more than in the south. In winter, the cyclonic eddies are beside the west coast and anticyclonic eddies on the east side in the Red Sea, while in summer it is the opposite. Also there is a noticeable change in some eddies from anticyclonic during winter to cyclonic during summer and vice versa in the north between 26.3° – 27.5°N. This study found that the FSM-SLA data near the coast is better than AVISO data and its estimated geostrophic currents are comparable to that of the CTD data.

Acknowledgments

The authors are deeply grateful to the data providers. JPL Physical Oceanography Distribution Active Archive Center (PODAAC), the Archiving Validation and Interpretation of Satellite Oceanographic (AVISO) to provide Jason-2 data. This also extends to the Saudi Arabian GCS for providing hourly tide gauge data along the coast of the Red Sea. They are thankful for the High-Performance Computing center at King Abdulaziz University (http://hpc.kau.edu.sa) for giving us a chance to use their facilities during analyses of data. Our thanks are for King Abdulaziz University, Jeddah, Saudi Arabia and Hodeidah University, Yemen for making this research possible.

References

Abdallah, A. M. and Eid, F. M.: On the steric sea level in the Red Sea, Int. Hydrogr. Rev., 66(1), 115–124., 1989.

Ahmad, F. and Sultan, S. A. R.: On the heat balance terms in the central region of the Red Sea, Deep Sea Res. Part A. Oceanogr. Res. Pap., 34(10), 1757–1760, 1987.

Ahmad, F. and Sultan, S. A. R.: Surface heat fluxes and their comparison with the oceanic heat-flow in the red-sea, Oceanol. Acta, 12(1), 33–36, 1989.

Al Saafani, M. A. and Shenoi, S. S. C.: Seasonal cycle of hydrography in the Bab el Mandab region, southern Red Sea, Proc. Indian Acad. Sci. Earth Planet. Sci., 113(3), 269–280, doi:10.1007/BF02716725, 2004.

Andersen, O. B. and Knudsen, P.: The role of satellite altimetry in gravity field modelling in coastal areas, Phys. Chem. Earth, Part A Solid Earth Geod., 25(1), 17–24, doi:10.1016/S1464-1895(00)00004-1, 2000.

Birol, F., Cancet, M. and Estournel, C.: Aspects of the seasonal variability of the Northern Current (NW Mediterranean Sea) observed by altimetry, J. Mar. Syst., 81(4), 297–311, doi:10.1016/j.jmarsys.2010.01.005, 2010.

Bower, A. and Farrar, J. T.: Air – Sea Interaction and Horizontal Circulation in the Red Sea, in The Red Sea the Formation, Morphology, Oceanography and Environment of a Young Ocean Basin, edited by N. M. A. Rasul and I. C. F. Stewart, pp. 329–342, Springer., 2015.

Chelton, U. B., Ries, J. C., Haines, B. J., FU, L.-L. and Callahan, P. S.: Satellite Altimetry and Earth Sciences, in Satellite Altimetry and Earth Sciences: A Handbook of Techniques and Applications, edited by L.-L. FU and A. Cazenave, pp. 1–122, Academic Press, San Diego, California ,USA., 2001.

Chen, C., Li, R., Pratt, L., Limeburner, R., Berdsley, R., Bower, A., Jiang, H., Abualnaja, Y., Xu, Q., Lin, H., Liu, X., Lan, J. and Kim, T.: Process modeling studies of physical mechanisms of the formation of an anticyclonic eddy in the central Red Sea, J. Geophys. Res. Ocean., 119, 1445–1464, doi:10.1002/2013JC009351, 2014.

Clifford, M., Horton, C., Schmitz, J. and Kantha, L. H.: An oceanographic nowcast/forecast system for the Red Sea, J. Geophys. Res. Ocean., 102(C11), 25101–25122, doi:10.1029/97JC01919, 1997.

Deng, X. and Featherstone, W. E.: A coastal retracking system for satellite radar altimeter waveforms : Application to ERS-2 around Australia, J. Geophys. Res., 111(C06012), 1–16, doi:10.1029/2005JC003039, 2006.

Deng, X., Featherstone, W. E., Hwang, C. and Shum, C. K.: Improved Coastal Marine Gravity Anomalies at the Taiwan Strait from Altimeter Waveform Retracking, in Proceedings of the International Workshop on Satellite Altimetry for Geodesy, Geophysics and Oceanography., 2001.

Desportes, C., Obligis, E. and Eymard, L.: On Wet Tropospheric Correction For Altimetry In Coastal Regions, in 'Envisat Symposium 2007',Montreux, Switzerland, pp. 23–27., 2007.

Durand, F., Shankar, D., Birol, F. and Shenoi, S. S. C.: Spatio-temporal structure of the East India Coastal Current from satellite altimetry, J. Geophys. Res. Ocean, 114(2), 18, doi:10.1029/2008JC004807, 2009.

Edwards, F. J.: Climate and oceanography, Red sea, 1, 45–68, 1987.

Eladawy, A., Nadaoka, K., Negm, A., Abdel-Fattah, S., Hanafy, M. and Shaltout, M.: Characterization of the northern Red Sea's oceanic features with remote sensing data and outputs from a global circulation model, Oceanologia, 59(3), 213–237, doi:10.1016/j.oceano.2017.01.002, 2017.

Eshel, G. and Naik, N. H.: Climatological Coastal Jet Collision, Intermediate Water Formation, and the General Circulation of the Red Sea, Am. Meteorol. Soc., 1233–1257, doi:10.1175/1520-0485, 1997.

Ghosh, S., Kumar Thakur, P., Garg, V., Nandy, S., Aggarwal, S., Saha, S. K., Sharma, R. and Bhattacharyya, S.: SARAL/AltiKa Waveform Analysis to Monitor Inland Water Levels: A Case Study of Maithon Reservoir, Jharkhand, India, Mar. Geod., 38(S1), 597–613, doi:10.1080/01490419, 2015.

Hwang, C., Guo, J., Deng, X., Hsu, H. Y. and Liu, Y.: Coastal gravity anomalies from retracked Geosat/GM altimetry: Improvement, limitation and the role of airborne gravity data, J. Geod., 80(4), 204–216, doi:10.1007/s00190-006-0052-x, 2006.

Johns, W. E., Jacobs, G. A., Kindle, J. C., Murray, S. P. and Carron, M.: Arabian marginal seas and gulfs, NAVAL RESEARCH LAB STENNIS SPACE CENTER MS OCEANOGRAPHY DIV., 1999.

Khaki, M., Forootan, E. and Sharifi, M. A.: Satellite radar altimetry waveform retracking over the Caspian Sea, Int. J. Remote Sens., 35(17), 6329–6356, 2014.

Manasrah, R., Badran, M., Lass, H. U. and Fennel, W.: Circulation and winter deep-water formation in the northern Red Sea, Oceanologia, 46(1), 5–23, 2004.

Manasrah, R., Hasanean, H. M. and Al-Rousan, S.: Spatial and seasonal variations of sea level in the Red Sea, 1958-2001, Ocean Sci. J., 44(3), 145–159, doi:10.1007/s12601-009-0013-4, 2009.

Mantripp, D.: Radar altimetry, in The Determination of Geophysical Parameters From Space, edited by N. . Fancey, I. . Gardiner, and R. A. Vaughan, p. 119, Institute of Physics Publishing, London, UK., 1966.

Morcos, S. A.: Physical and chemical oceanography of the Red Sea, Ocean. Mar. Biol. Ann. Rev, 8, 73–202, 1970.

Murray, S. P. and Johns, W.: Direct observations of seasonal exchange through the Bab el Mandab Strait, Geophys. Res. Lett., 24(21), 2557–2560, 1997.

Neumann, A. C. and McGill, D. A.: Circulation of the Red Sea in early summer, Deep Sea Res., 8(3–4), 223–235, 1961.

Osman, M.: Evaporation from coastal water off Port-Sudan, J. King Abdulaziz Univ. Mar. Sci., 17(4), 1–2, 1985.

Patzert, W. C.: Wind-induced reversal in Red Sea circulation, Deep Sea Res., 21(2), 109–121, 1974

Phillips, O. M.: On turbulent convection currents and the circulation of the Red Sea, Deep Sea Res., 13(6), 1149–1160, 1966.

Quadfasel, D. and Baudner, H.: Gyre-scale circulation cells in the Red-Sea, Oceanol. Acta, 16(3), 221–229, 1993.

Siedler, G.: General circulation of water masses in the Red Sea, in Hot Brines and Recent Heavy Metal Deposits in the Red Sea, edited by E. T. Degens and D. A. Ross, pp. 131–137, Springer, New York., 1969.

Smeed, D. A.: Exchange through the Bab el Mandab, Deep Sea Res. Part II Top. Stud. Oceanogr., 51(4), 455–474, 2004.

Sofianos, S. and Johns, W. E.: Water mass formation, overturning circulation, and the exchange of the Red Sea with the adjacent basins, in The Red Sea the Formation, Morphology, Oceanography and Environment of a Young Ocean Basin, edited by N. M. A. Rasul and I. C. F. Stewart, pp. 343–353, Springer., 2015

Sofianos, S. S. and Johns, W. E.: An Oceanic General Circulation Model (OGCM) investigation of the Red Sea circulation : 2 . Three-dimensional circulation in the Red Sea, J. Geophys. Res., 108, 1–15, doi:10.1029/2001JC001185, 2003.

Sofianos, S. S. and Johns, W. E.: An Oceanic General Circulation Model (OGCM) investigation of the Red Sea circulation, 1. Exchange between the Red Sea and the Indian Ocean, J. Geophys. Res., 107(C11), 3196, doi:10.1029/2001JC001184, 2002.

Sofianos, S. S. and Johns, W. E.: Observations of the summer Red Sea circulation, J. Geophys. Res., 112, 1–20, doi:10.1029/2006JC003886, 2007.

Sofianos, S. S. and Johns, W. E.: Wind induced sea level variability in the Red Sea, Geophys. Res. Lett., 28(16), 3175–3178, 2001.

Sultan, S. and Ahmad, F.: Geostrophic Currents in the Central Part of the Red-Sea during Early Summer, Oceanol. Acta, 13(3), 397–401, 1990.

Sultan, S. A. R. and Elghribi, N. M.: Sea level changes in the central part of the Red Sea, Indian J. Mar. Sci., 32(2), 114–122, 2003.

Sultan, S. A. R., Ahmad, F. and Nassar, D.: Relative contribution of external sources of mean sea-level variations at Port Sudan, Red Sea, Estuar. Coast. Shelf Sci., 42(1), 19–30, 1996.

Taqi, A. M., Al-Subhi, A. M. and Alsaafani, M. A.: Extension of Satellite Altimetry Jason-2 Sea Level Anomalies Towards the Red Sea Coast Using Polynomial Harmonic Techniques, Mar. Geod., doi:10.1080/01490419.2017.1333549, 2017.

Tragou, E. and Garrett, C.: The shallow thermohaline circulation of the Red Sea, Deep Sea Res. Part I Oceanogr. Res. Pap., 44(8), 1355–1376, 1997.

Vignudelli, S., Cipollini, P., Astraldi, M., Gasparini, G. P. and Manzella, G.: Integrated use of altimeter and in situ data for understanding the water exchanges between the Tyrrhenian and Ligurian Seas, J. Geophys. Res., 105(C8), 19649–19664,doi:10.1029/2000JC900083, 2000.

Vignudelli, S., Cipollini, P., Roblou, L., Lyard, F., Gasparini, G. P., Manzella, G. and Astraldi, M.: Improved satellite altimetry in coastal systems : Case study of the Corsica Channel (Mediterranean Sea), Geophys. Res. Lett., 32(L07608), 1–5, doi:10.1029/2005GL022602, 2005.

Yao, F., Hoteit, I., Pratt, L. J., Bower, A. S., Zhai, P., Kohl, A. and Gopalakrishnan, G.: Seasonal overturning circulation in the Red Sea: 1. Model validation and summer circulation, J. Geophys. Res. Ocean., 119, 2238–2262, doi:10.1002/2013JC009331, 2014a.

Yao, F., Hoteit, I., Pratt, L. J., Bower, A. S., Köhl, A., Gopalakrishnan, G. and Rivas, D.: Seasonal overturning circulation in the Red Sea: 2. Winter circulation, J. Geophys. Res. Ocean., 119(4), 2263–2289, doi:10.1002/2013JC009331, 2014b.

Zhan, P., Subramanian, A. C., Yao, F. and Hoteit, I.: Eddies in the Red Sea: A statistical and dynamical study, J. Geophys. Res. Ocean., 3909–3925, doi:10.1002/2013JC009563, 2014.